II International Conference on Particle-based Methods – Fundamentals and Applications
PARTICLES 2011
E. Oñate and D.R.J. Owen (Eds)

3D VIRTUAL LABORATORY FOR GEOTECHNICAL APPLICATIONS: ANOTHER PERSPECTIVE

V. ROUBTSOVA*, M. CHEKIRED*, B. MORIN*, and M. KARRAY†

* Hydro-Quebec Research Institute
1800, boul. Lionel-Boulet, Varennes (Québec)
Canada J3X 1S1
bureau.accueil@ireq.ca, www.ireq.ca

† Université de Sherbrooke
Department of Civil Engineering, Faculty of Applied Sciences
2500 boulevard de l'Université, Sherbrooke (Québec)
Canada J1K 2R1
mourad.karray@usherbrooke.ca, www.usherbrooke.ca/gcivil/

Key Words: DEM, Cohesionless Soils, Shear Tests, OpenCL, OpenGL, Alioscopy.

Abstract.

Discrete element methods are important tools for investigating the mechanics of granular materials. In two dimensions, the reliability of these numerical approaches is increasingly being challenged, because they cannot take into account all the factors involved in the behavior of a granular medium.

With new concepts, such as high performance parallel computing and 3D visualization, it is now possible to conduct numerical simulations of granular materials made up of several thousands of particles, and also to follow the evolution of the various parameters involved in the behavior of a granular medium. Experimental tests have been carried out to validate the results obtained by using a virtual laboratory. This paper presents the earlier results obtained in our 3D Virtual Laboratory on the response of specimens of glass beads of uniform size during shear tests. Good agreement was achieved between the virtual simulations and the experimental tests.

This work highlights the possibility of using a new 3D virtual laboratory for dynamic simulation. This approach could be of significant value in improving the verification, validation, and communication of the simulation results of discrete element methods, which can in turn make the simulations more credible and thus useful in decision making.

1 INTRODUCTION

The direct shear test is widely used to measure the bulk material properties required to design many engineering problems, such as foundations, retaining walls, slab bridges, pipes, sheet piling, etc. Several attempts to numerically model this test in 2D have been conducted. However, the results obtained to date have often been marred by uncertainty, and so this 2D approach is not yet widely used. In addition, attempts are rarely made to validate the experimental results obtained by numerical modeling, and have often not been conclusive enough to impress practitioners. Computer hardware limitations have also slowed its widespread acceptance. In order to overcome these difficulties, a parallel computation approach has been used to develop a dynamic 3D numerical code (called SIMSols). The OpenCL framework was used in order to achieve a high level of data parallelism on NVIDIA Graphics Processing Unit (GPU) based Tesla High Performance Computing (HPC) hardware. Using the OpenGL Application Programming Interface (API) and Alioscopy technology, autostereoscopic visualization is proposed. This paper presents the results obtained experimentally on a series of shear tests carried out on samples made up of glass beads, which helped validate the virtual laboratory results.

2 DIRECT SHEAR TEST

The direct shear test is one of the oldest soil strength tests performed in the laboratory. Even though this test has some disadvantages, which are documented in ASTM D 3080 – 98 [1], this test is routinely used by geotechnical engineers to determine the shear strength parameters of soil that are essential for stability assessment. The first direct shear apparatus was built by Alexander Collin in 1846 to measure the strength of a clay soil shear to study the stability of slopes [2, 3, 4]. The current version of the direct shear apparatus was designed by Casagrande in 1932.

A normal load is applied to the specimen and the specimen is sheared across the pre-determined horizontal plane between the two halves of the shear box. Measurements of shear load, shear displacement and normal displacement are recorded. From the results, the shear strength parameters can be determined. Figure 1 shows a schematic representation of the shear box.

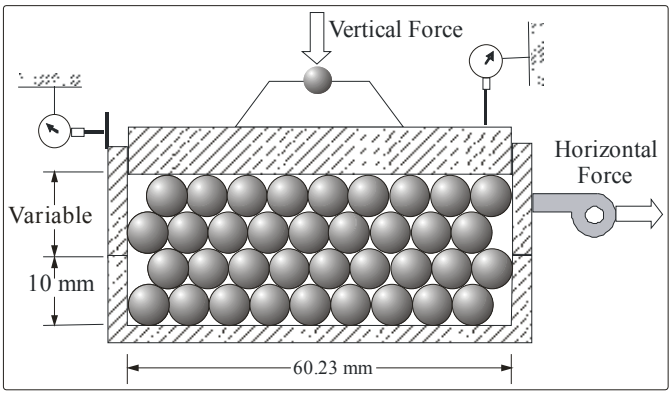

Figure 1: Schematic representation of a shear box

3 DISCRETE ELEMENT METHOD SIMULATIONS

The Discrete Element Method (DEM), proposed by Cundall and Strack [5], is a powerful tool for numerical modeling of the mechanical behaviour of a large number of particles. Each particle is considered as a rigid body with translational and rotational degrees of freedom assigned to their centers of mass. An explicit time integration scheme, based on Newton's second law, is applied to the equations of motion to keep track of the particle positions and velocities. While moving, some of the particles will come into contact with one another. To address this issue, a contact formulation is required to apply repulsive forces to prevent the particles from moving through each other.

In spite of the progress made to date, practitioners in fields such as granular materials science, geotechnical, mining, the food industry, etc. still lack confidence in this method, and, as a result, further development is required. In the geotechnical field, for example, the major concern is the prohibitive computational time it requires, and another is the non representativeness of the 2D approach in evaluating the various phenomena encountered in dense granular materials. In fact, modeling 2D fails to take into account all of the involved parameters. This has been confirmed by several studies, including that of Sallam [6], who observed that the dilatancy of the 2D model is greater than that observed experimentally. Sallam attributes this difference to the fact that, in 2D simulations, particles cannot benefit from the level of freedom that 3D offers. In terms of the contact between particles, Masson et and Martinez [7] simulated granular material confined in a gallery and subjected to a horizontal thrust. Their simulation was conducted in both 2D and 3D. The results show that the 3D model allows a compaction and displays significantly more contacts than a 2D model. On the other hand, by comparing experimental results on Daytona Beach sand and on rounded materials with those obtained by numerical simulations, Das [8] found that the 2D simulations underestimate the results for both materials. The angle of internal friction of Daytona Beach sand obtained from 2D simulations was 27^{o}, while that obtained from 3D simulations varies from 39 to 43^{o}, which is close to the experimental value of 37.40^{o}. For rounded materials, the angle of internal friction obtained from 2D simulations was 17.2^{o}, while that obtained from 3D simulations varies from 25^{o} to 26.6^{o}, which is within the internal friction angle range of 24.4^{o} to 27^{o}, as reported in the literature by O'Sullivan et al. [9] and Phillips et al. [10].

Finally, while there are numerous publications describing the potential of DEM, only a small number of studies in the geotechnical field have been validated by experimental results [11].

A further concern is particle shape. It is well known that the geometry of real soil particles is not adequately represented by spheres, and that samples formed of spherical particles cannot represent the complexity of soil behavior. Attempts to simulate soils with particles of simple non spherical form in 2D began to be considered in the last decade [6, 12] and in 3D [13, 14].

4 THE MOTION AND INTERACTION OF PARTICLES (DEM)

The motions of particle *i* caused by its interactions with neighbouring particles is described by the equations:

$$\begin{aligned} m_i \frac{d\vec{V}_i}{dt} &= m_i \vec{g} + \sum_{j=1}^{k} \left(\vec{F}_{cn,ij} + \vec{F}_{dn,ij} + \vec{F}_{ct,ij} + \vec{F}_{dt,ij} \right) + \vec{F}_{fl} \\ I_i \frac{d\vec{\omega}_i}{dt} &= \sum_{j=1}^{k} \left(\vec{T}_{ij} + \vec{M}_{ij} \right) + \vec{M}_{fl} \end{aligned} \tag{1}$$

where:

m_i and I_i are the mass (kg) and moment of inertia (kg·m^2) of particle *i* respectively;

$\vec{V}_i$ and $\vec{\omega}_i$ are the translational (m/s) and rotational (s^{-1}) velocities of particle *i* respectively;

k is the number of neighboring particles;

$\vec{F}_{cn,ij} = -K_n \delta_n^{\frac{3}{2}} \vec{n}$ is the normal force of contact (N);

$\vec{F}_{dn,ij} = -C_n \vec{V}_{n,ij}$ is the normal damping force (N);

$\frac{d\vec{F}_{ct,ij}}{\vec{d}\delta_t} = -K_t$ is the tangential force of contact (N), the value of which is limited by $\left|F_{ct,ij}\right| \le \mu_s F_{cn,ij}$;

$\vec{F}_{dt,ij} = -C_t \vec{V}_{t,ij}$ is the tangential damping force (N);

$\vec{F}_{fl}$ is the drag force (N);

$\vec{T}_{ij} = R_i \left(\vec{F}_{ct,ij} + \vec{F}_{dt,ij} \right)$ is the torque moment (N·m);

$\vec{M}_{ij} = -\mu_r \left| \vec{F}_{cn,ij} \right| \frac{\vec{\omega}_i}{\left|\vec{\omega}_i\right|}$ is the friction torque (N·m);

$\vec{M}_{fl}$ is the drag moment (N·m);

$K_n = \frac{4}{3} E^* \sqrt{R^*}$, $C_n = -\frac{\ln \varepsilon \sqrt{m^* K_n}}{\sqrt{\pi^2 + (\ln \varepsilon)^2}}$, $K_t = 2\sqrt{R\delta_n} \left(\frac{G_i}{2-\nu_i} + \frac{G_j}{2-\nu_j} \right)$, $C_t = K_n \sqrt{\frac{K_t}{K_n}}$;

δ_n and δ_t are the normal and tangential contact displacement respectively:

$\frac{1}{E^*} = \frac{1-\nu_i^2}{E_i} + \frac{1-\nu_j^2}{E_j}$ and $\frac{1}{R^*} = \frac{1}{\left|R_i\right|} + \frac{1}{\left|R_j\right|}$

where E is Young's modulus (Pa), ν is the Poisson ratio, R_i is the particle radius (m), and μ_s, μ_r are the sliding and rolling (m) friction coefficients respectively, and ε is the restitution coefficient. The determination of interaction forces has been detailed by Lee et al. [15], Zhou et al. [16], and Nakashima [17].

5 EXPERIMENTAL PROCEDURE

The experimental shear tests were carried out in a 60.23 x 60.07 mm shear box (Figure 1). Samples made up of glass beads of uniform size were placed so as to have the maximum number of beads of glass per layer. However, because of the uniformity of the size of the glass beads, it is not always possible to fill the box so that there is no clearance between the rows of beads and the ends of the box. That is why, as we see in Figure 2, there is clearance between the glass bead row and the box (at the left-hand side and at the top). The size of this gap varies with the size of the beads, and it is distributed along the length and width of the sample during placement of the next row or when the load is applied. As a result, to facilitate the numerical modeling of the samples in the virtual laboratory, the glass beads have been placed so as to have the same number of glass beads per layer. Knowing the size of the glass beads and the length and width of the box, it is possible to determine the size of the gap between the rows of beads and the ends of the box, and thus simulate the arrangement of the glass beads during modeling. A special effort was made to ensure the appropriate placement of the glass beads in the shear box model. The glass bead diameter and the number of rows used for each size of glass bead are listed in Table 1. Table 2 presents the mechanical properties of the glass beads used.

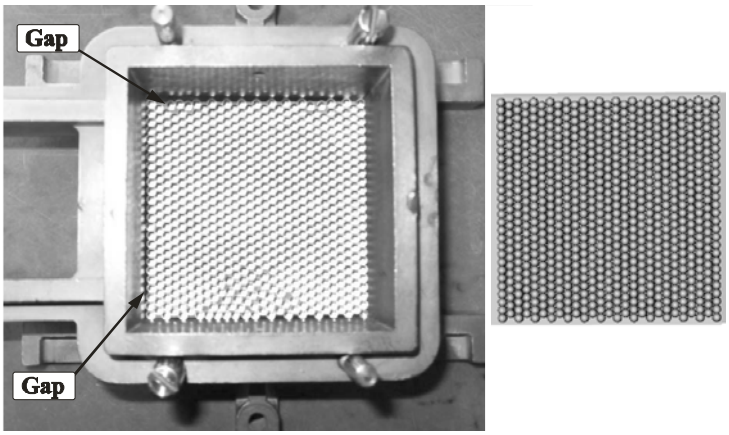

Figure 2: Photograph of the first layer of glass beads: (a) in the shear box; and (b) used for modeling

Table 1: Glass bead diameter and number of rows

Test	1	2	3	4	5
Glass bead diameter (mm)	2.38125	3.175	3.96875	4.7625	6.35
Number of layers	8	6	5	4	4

Table 2: Mechanical properties of the glass beads

Mechanical properties	Value
Young's Modulus	62.784 GPa
Poisson Ratio	0.2
Density	2230 kg/m^3
Coefficient of Restitution	0.87
Sliding Friction	0.02
Coefficient of Rolling Friction	$5 \cdot 10^{-5}$ m

6 PARALLELIZATION

Typically, numerical simulations using DEM are computationally intensive, either because they take a long time to complete or because they require access to substantial computing resources. In order to keep both simulation time and computational resource requirements to a minimum, the model was parallelized using GPU (Graphics Processing Units). Modern GPU are massive data parallel processors capable of handling over 500 billion operations per second, which makes them well suited to handling data bounded problems such as DEM simulations. Initial development was carried out on a 6 GB, 448 core Tesla M2070 GPU from Nvidia [18]. This particular card was chosen for its relatively large amount of memory, in order to reduce the amount of costly memory movement across the PCIe. For portability, we chose the OpenCL (Open Computing Language) framework [19], which offers an abstract view of the parallel architecture used. This allowed us to use both the CPU (Central Processing Units) and the GPU backend. OpenCL represent the data space as an n dimensional NDRange. This space is divided into work groups, which are then subdivided into fine grain work items. The Nvidia Fermi architecture divides compute cores among SM (Streaming Multiprocessors), which consist of blocks of 32 lock-stepped CUDA cores. Each particle interaction calculation was assigned to an OpenCL work item, which was then computed on an individual Cuda core.

7 VISUALIZATION

The visualization of large scale particle-to-particle interaction simulations poses multiple challenges. The sheer volume of data imposes either multiple static representations or a dynamic view, in order to permit observation of the entire system. In order to circumvent the problem of occluded particles, a dynamic 3D view of the model was chosen. Both classic 2D projection with transparency and the glass free autostereoscopic visualization approach were implemented. Using Alioscopy technology, we were able to project eight different perspectives on a screen covered by a lenticular array, resulting is seven simultaneously observable angles of vision. This technology allows multiple observers to interact with a simulation, and permits more complex systems to be viewed. The OpenGL (Open Graphics Library) API (Application Programming Interface) [20] was used to compute both the flat projection, as well as the different views required by the Alioscopy technology in a portable manner. GLSL (Graphics Library Shading Language) shaders were used to combine the

views into a single image projected on the screen, which is then redecomposed into individual images by the lenticular lens. OpenCL-OpenGL integration allows the reuse of particles from within the model without having to transfer data back to main memory.

The visualization plays an important role in the validation of numerical algorithms. It can help verify the correctness of the physical ideas used in the numerical modeling. It can also can show paths that could not otherwise be considered, given the large datasets created during a computer simulation.

8 TEST RESULTS

A total of 20 shear tests were performed under vertical loads of 50 kPa, 160 kPa, 280 kPa, and 400 kPa on spherical glass beads of uniform size to validate the virtual laboratory results. In an attempt to verify the predictive capability of the DEM, closely matching 3D discrete element simulations of the shear tests were performed and compared with the experimental observations. Figures 3 to 7 show the results obtained, and the ability of the numerical simulation to capture the macroscopic response of the sample's behaviour during the tests. However, the post peak response reveals differences, which can be attributed to the chaotic movement of the glass beads during testing.

These differences may be caused by one or more of the following uncertainties associated with the DEM hypothesis and with the experimental testing that are not accounted for in the model:

- The non sphericity of the glass beads that are assumed to be perfect spheres. The spheres used in the numerical modeling are perfect;
- The location of individual glass beads. To reproduce the exact location of every bead, a photograph of each layer was taken to reproduce that location precisely in the simulations. However, given that there is a clearance between the row of glass beads and the walls of the shear box, it is impossible to know the movement of every glass bead precisely when loads are applied;
- The small bead fragments resulting from breakage at the surface of the glass beads can influence their macroscopic behaviour. We can observe (Figure 8) the surface conditions before and after the tests;
- The large degree of uncertainty in the mechanical properties of the bead system;
- The contact formulation;
- The simulated particles are allowed to virtually overlap one another at contact points, as they are regarded as rigid bodies whereas in reality the particles deforms on contact;
- The main input parameters in the numerical model (i.e. normal and tangential stiffness, and a damping coefficient).

In terms of visualization possibilities, figure 9 shows four different shearing steps, and figure 10 depicts the intensity of the forces of contact between the particles.

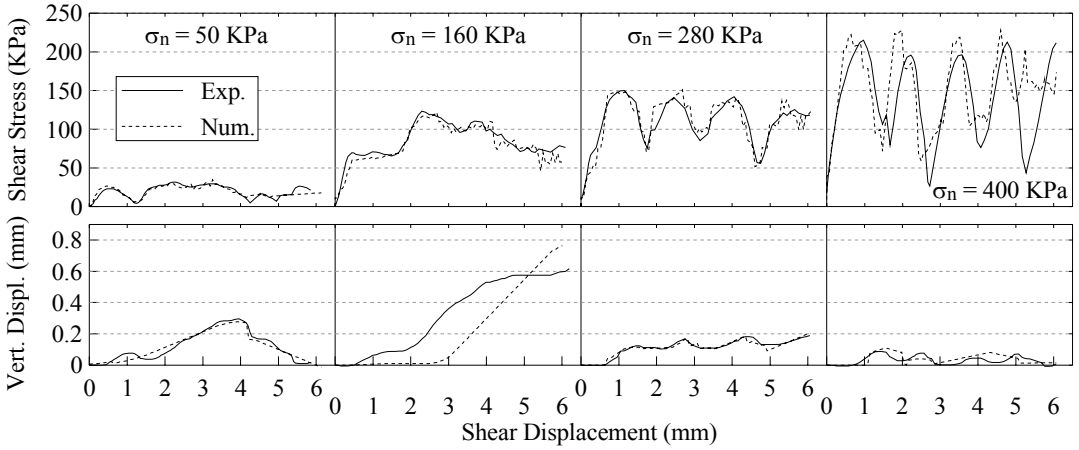

Figure 3: Experimental and numerical results on samples made up of glass beads 2.38125 mm diameter

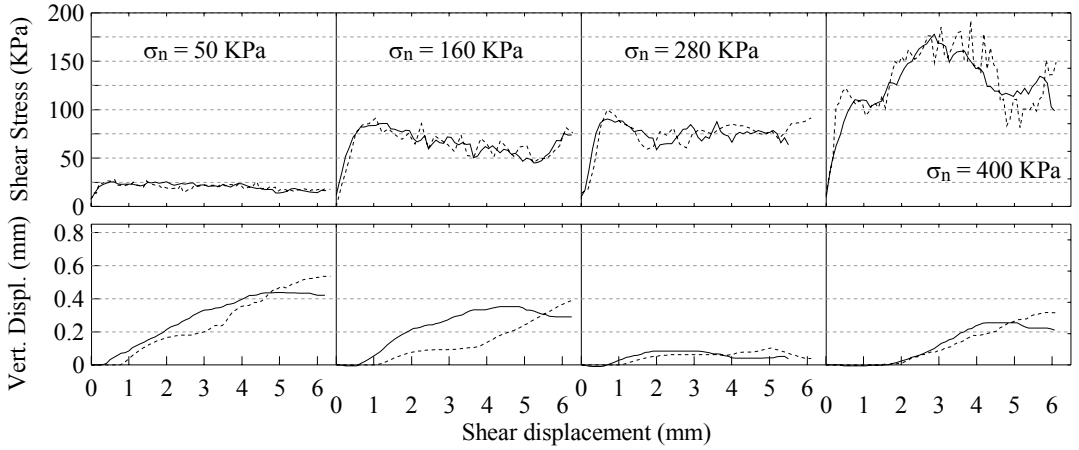

Figure 4: Experimental and numerical results on samples made up of glass beads 3.175 mm diameter

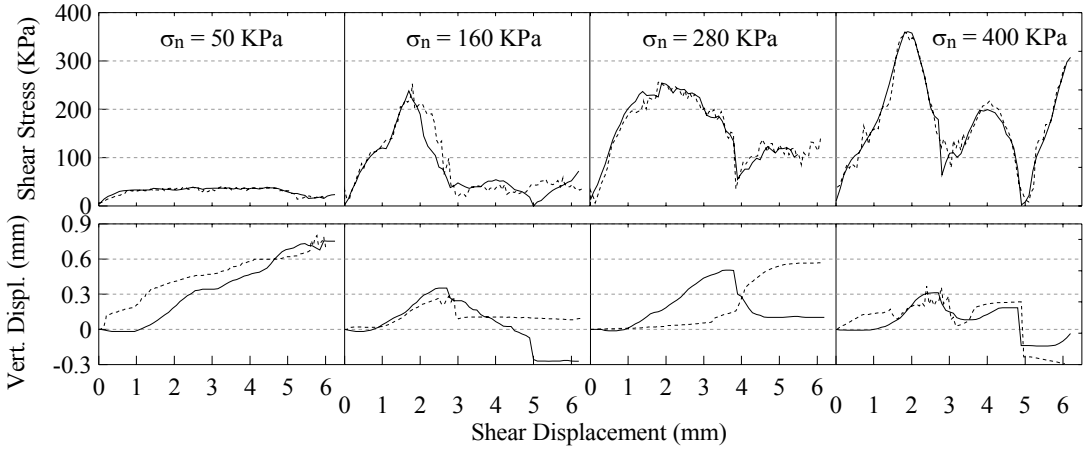

Figure 5: Experimental and numerical results on samples made up of glass beads 3.96875 mm diameter

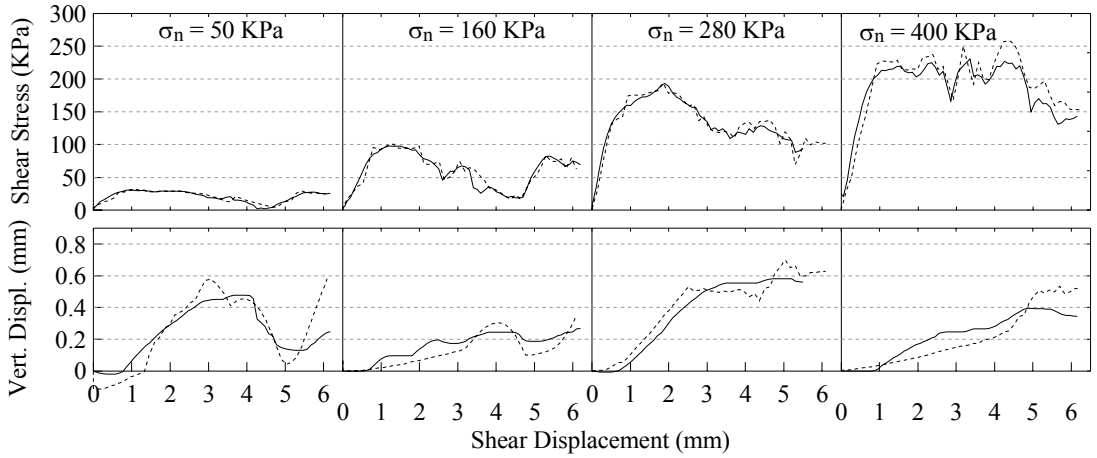

Figure 6: Experimental and numerical results on samples made up of glass beads 4.7625 mm diameter

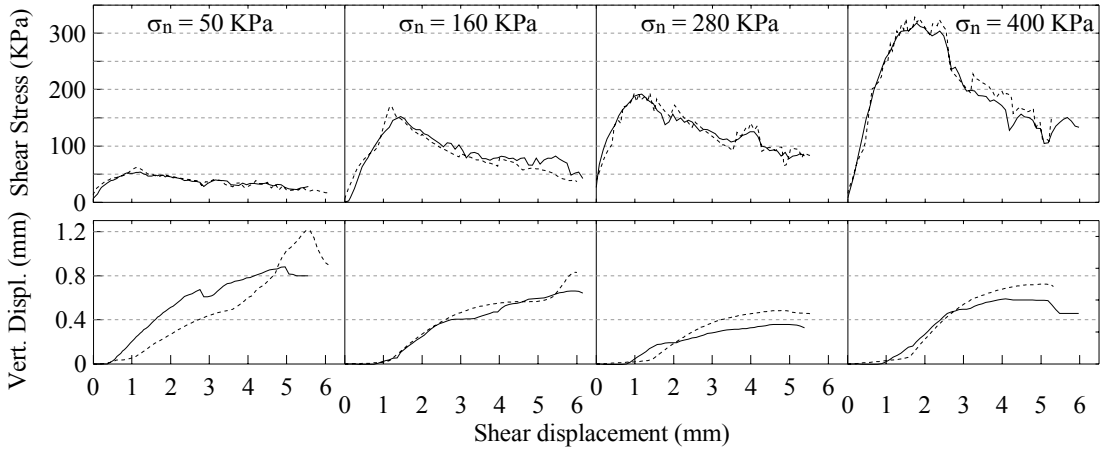

Figure 7: Experimental and numerical results on samples made up of glass beads 6.35 mm diameter

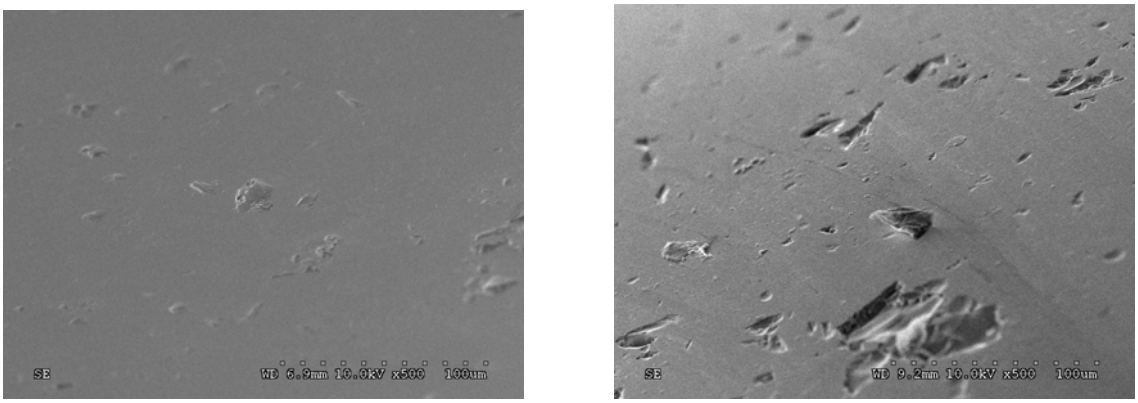

Figure 8: A closer view of a glass bead surface: (a) before and (b) after the shear tests

9 FUTURE WORK

A number of research projects are planned with the aim of developing our 3D Virtual Laboratory. Some of the topics of these projects are the following:

- Validation of the numerical results obtained by our 3D Virtual Laboratory for experimental shear tests carried out without clearance between the shear box and the glass beads;
- Validation of the numerical results obtained by our 3D Virtual Laboratory for various experimental tests on samples with the same grain size as they have in reality;
- Improvement of the capacity of our 3D Virtual Laboratory to understand the various phenomena encountered in the geotechnical field at the particle scale;
- Optimization of the various algorithms used in our 3D Virtual Laboratory, in order to reduce calculation times;
- Study of the sensitivity of the coefficients used in numerical simulations;
- Study of the effects of scale;
- Study of the influence on macroscopic behaviour of the water menisci between neighboring grains.

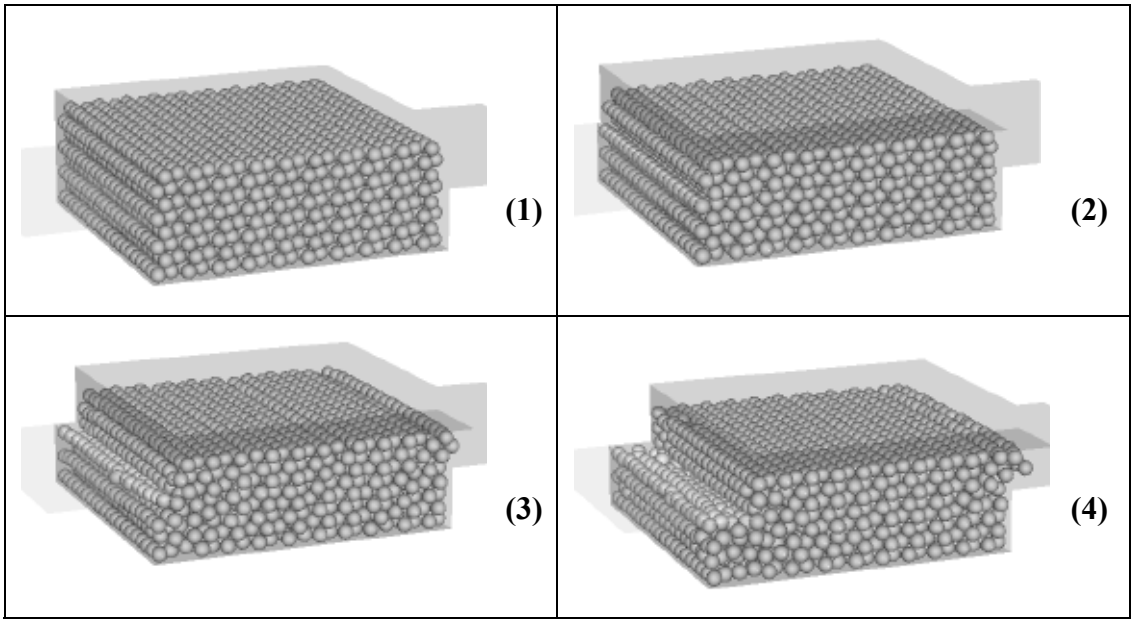

Figure 9: Example of the 3D visualization of four shearing steps (Glass bead diameter = 2.38125 mm)

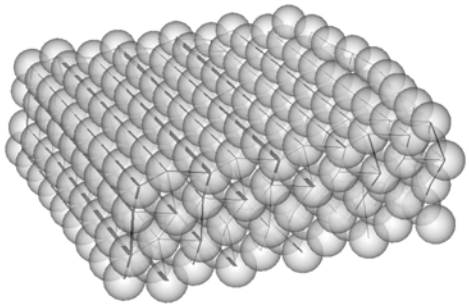

Figure 10: 3D visualization of the contact force between particles

10 CONCLUSION

The earlier work performed in our 3D Virtual Laboratory is presented in this paper. This laboratory was developed to meet needs encountered in the geotechnical field. The example presented in this article concerns only direct shear testing. The experimental and numerical results are in good agreement. Several factors explain the small differences, among them the locations of the glass beads during the trials and the inaccuracy of the coefficients used.

Our 3D Virtual Laboratory has the capacity to reproduce the shear tests on samples made up of glass beads, but also enables visualization of particle behaviour at macroscopic and particle level in 3D. This makes 3D simulation very practical from a quantitative standpoint.

REFERENCES

[1] ASTM D3080 -98 (2004) ASTM D3080: Standard test method for direct shear test of soils under consolidated drained conditions.

[2] Collin, A. (1846). Recherches expérimentales sur les glissements spontanés des terrains argileux. Carilian-Goeurley et Delmont, Paris.

[3] Skempton, A.W. (1945). "A slip in the west bank of the Eau Brink Cut". *Jour. Instn. Civil Engrs*., Vol.24, pp.267-287.

[4] Skempton, A.W., 1985. Residual strength of clays in landslides, Folded Strata and the Laboratory. *Geotechnique,* Vol. 35, 3–18.

[5] Cundall, P. and Strack, O. (1979). "A Discrete numerical model for granular assemblies." *Geotechnique*. Vol. 29(1): 47-65.

[6] Sallam, A.M. (2004). Studies on modeling angular soil particles using the discrete element method. *Ph.D. Thesis*, University of South Florida, Tampa, FL.

[7] Masson, S. and Martinez, J. (2000). Multiscale simulations of the mechanical behaviour of an ensiled granular material. *Mechanics of Cohesive-Frictional Materials 5* (6), 425–442.

[8] Das, N. (2007) Modeling three-dimensional shape of sand grains using Discrete Element Method. *Ph.D Thesis*, University of South Florida. 149 p.

[9] O'Sullivan, C. Bray, J. D. and Riemer, M. (2004), Examination of the response of regularly racked specimens of spherical particles using physical tests and discrete elements simulations. *Journal of Engineering Mechanics*. p.1140 – 1150.

[10] Phillips, J. C., Hogg, A.J., Kerswell, R.R. and Thomas, N.H. (2006) Enhanced mobility of granular mixtures of fine coarse particles, *Earth and Planetary Science letters*. No 246. p. 466-480.
[11] Munjiza, A. (2010) Proceedings of the 5th International Conference on Discrete Element methods – *Simulations of Discontinua: Theory and Applications* (London). 551 p.
[12] Ashmaw, A. K., Sukumaran, B. and Hoang, A. V. (2003) Evaluating the influence of particles shape on liquefaction behaviour using discrete element method. *Thirteenth International Offshore and Polar Engineering Conference (ISOPE 2003)*. Honolulu, Hawaii. 8p.
[13] Wellmann, C., Lillie, C. and Wriggers, P.: (2008) Comparison of the macroscopic behavior of granular materials modeled by different constitutive equations on the microscale. *Finite Elements Anal Design*, Vol. 44, 259–271 (2008).
[14] Yan, Y.and Ji, S. (2010) Discrete element method of direct shear tests for a granular material. *International Journal for Numerical and Analytical Methods in Geomechanics*. Vol. 34, 978-990.
[15] Lee, H., Kwon, J. H., Kim, K. H. and Cho, H. C., (2008), "Application of DEM model to breakage and liberation behaviour of recycled aggregates from impact-breakage of concrete waste." *Minerals Engineering*. Vol 21: 761-765.
[16] Zhou, Y. C., Xu, B. H., Yu, A. B., and Zulli, P. (2002). "An experimental and numerical study of the angle of repose of coarse spheres." *Powder Technology.* Vol. 125: 45-54.
[17] Nakashima H. (2004). "Discrete Element Method (DEM) and its possible application." *SICE Annual Conference in Sapporo, Japan*. Vol. 2: 1104-1107.
[18] NVIDIA Corporation (2009), NVIDIA's Next Generation CUDA Compute Architecture: *Fermi, NVIDIA Corporation*.
[19] Munshi, A. (2011) The OpenCL Specification Version 1.1, The Khronos Group.
[20] Mark, S. and Akeley, K., (2010) The OpenGL Graphics System: A Specification Version 4.1 (Core Profile), *The Khronos Group*.